# One-pot synthesized MoC imbedded in ordered mesoporous carbon as a catalyst for $N_2H_4$ decomposition†

Hui Wang,[ab] Aiqin Wang,[a] Xiaodong Wang[a] and Tao Zhang*[a]

**Nanosized and highly dispersed molybdenum carbide was fabricated in the carbon walls, along with the formation of ordered mesoporous carbons, *via* a one-pot organic–organic cooperative self-assembly approach.**

Transition metal carbides, in particular molybdenum and tungsten carbides, are promising catalytic materials for replacing precious metal catalysts in a variety of industrially important reactions.[1] Generally speaking, in order to obtain a desired catalytic activity and stability, the low-surface-area pure carbides have to be supported on large-surface-area carriers such as alumina, silica or carbon. In particular, when carbon materials are employed as the supports, the transition metal carbides can be formed *in situ via* carbothermal reduction.[2] In that case, utilization of external carbon sources such as hydrocarbons becomes unnecessary, and possible carbon deposition on the catalyst surface can be effectively avoided.[3] However, for this kind of *in situ* synthesis of metal carbide/carbon composites, ordered mesoporous carbons have not been used as the support so far. Moreover, the synthesis process usually involves impregnating of the carbon support with metal precursors, followed by calcination and carbothermal reduction, such that the carbides will be formed just on the carbon surface, and will not be incorporated into the carbon framework. Unfortunately, under certain severe reaction conditions, aggregation or sintering of the metal carbide nanoparticles would occur, resulting in the loss of activity. Previous work by several research groups[4] have shown that, by imbedding metal particles in the carbon walls of ordered mesoporous carbon, thermally stable and catalytically active catalysts could be obtained. More recently, Lu *et al.*[5] have found that molecular-level Pd clusters dispersed in the carbon walls could be synthesized by pyrolyzing composites containing Pd and carbon precursors in the pores of SBA-15. The resultant catalyst was highly selective for alcohol oxidation. On the other hand, Su *et al.*[6] have reported that ordered mesoporous carbon could act both as the support and the reducing agent for ruthenium nanoparticles, and the intimate interfacial contact between the Ru nanoparticles and the carbon support was believed to be responsible for the remarkably high catalytic activity and stability in the hydrogenation of benzene and toluene. The above studies suggest that the imbedding of active component in carbon walls and the generating of a strong interaction between the active component and the support would help to yield a thermally stable and highly active catalyst. However, they all involve a nanocasting procedure which is a very fussy, high-cost and thus industrially unfeasible method.[7] Recently, ordered mesoporous carbons (OMCs) have been successfully fabricated *via* a sol-gel organic–organic self-assembly strategy similar to that for ordered mesoporous silicates.[8] This approach not only allows mass production of the OMCs, but also provides unique possibilities for incorporating other functional materials into the carbon frameworks by a facile one-pot procedure. Based on these ideas, we have designed and prepared MoC–OMC catalysts for hydrazine decomposition *via* a one-pot organic–organic cooperative self-assembling procedure. The synthesis involved introduction of the Mo precursor into the reaction mixture containing a resin and a surfactant. Interaction between the $Mo_7O_{24}^{6-}$ and the resin caused the Mo species to be incorporated into the framework of the resin, which in turn was self-assembled into an ordering structure under the direction of the surfactant. After being subjected to pyrolysis at a high temperature, the Mo ions were gradually reduced by the carbon to form MoC nanoparticles which were strongly imbedded in the carbon walls and were thereby thermally stable. Catalytic tests showed that the MoC–OMC composite was highly active for the decomposition of hydrazine.

In a typical synthesis, 5.0 g of F127 was dissolved in a solution containing 20.0 g of water and 16.0 g of ethanol under magnetic stirring, to which 3.3 g of resorcinol and 0.4 g of HCl (37 wt%) were added and stirred at room temperature until the solution became light yellow. Then, 0.3 g of ammonium heptamolybdate $((NH_4)_6Mo_7O_{24}\cdot4H_2O)$ was added to the above solution and the mixture was continuously stirred for 2 h. After that, 4.9 g of formaldehyde (37 wt%) was added, and the solution became green in colour. The solution was allowed to stand at room temperature for one week, until it separated completely into two layers. The colourless upper layer was discarded, while the green-coloured and polymer-rich lower phase was cured at 85 °C for 5 days, and then it was pyrolyzed under a nitrogen atmosphere at 800 °C for 3 h, with a heating rate of 2 °C min$^{-1}$. The resulting composite was denoted as MoC–OMC. For comparison, pure OMC was synthesized exactly the same as the above procedure, but without the addition of the molybdenum precursor. A $Mo_2C$/OMC composite was also obtained by incipient wetness impregnating the OMC with an aqueous solution of ammonium heptamolybdate, followed by drying at 120 °C and carburizing at 800 °C for 3 h in nitrogen.

[a] *State Key Laboratory of Catalysis, Dalian Institute of Chemical Physics, Chinese Academy of Sciences, PO Box 110, Dalian, 116023, P.R. China. E-mail: taozhang@dicp.ac.cn; Fax: +86-411-84691570; Tel: +86-411-84379015*
[b] *Graduate University of Chinese Academy of Sciences, Beijing, 100049, P.R. China*
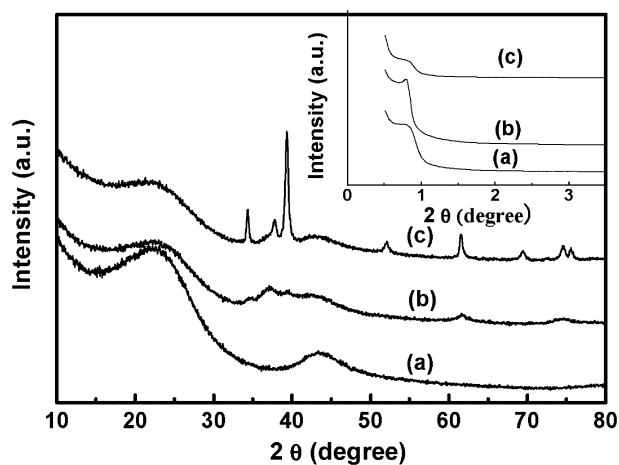
**Fig. 1** Low-angle (inset) and wide-angle XRD patterns of (a) OMC, (b) MoC–OMC and (c) Mo₂C/OMC.

Fig. 1 shows the X-ray diffraction (XRD) patterns of the MoC–OMC, Mo₂C/OMC and OMC. In the low angle range (inset), a diffraction peak could be clearly seen on the three samples, which can be indexed as a [100] reflection of a hexagonal mesostructure. It can be noted that the peak intensity of the MoC–OMC is higher than those of the other two samples. This may be caused by the increased contrast between the X-ray scattering from the walls to that of the empty pores, suggesting that the MoC particles in the MoC–OMC were incorporated into the carbon walls, rather than in the pores. In contrast, by comparing the low-angle XRD pattern of the Mo₂C/OMC with that of the OMC, the peak intensity of the Mo₂C/OMC was found to be slightly weaker than that of the OMC, implying that the structure of the preformed OMC was partially destroyed by the doping of the Mo₂C.

On the other hand, the wide-angle XRD patterns varied greatly with the introduction of the Mo species. For the OMC sample, two broad diffraction peaks centered at 22.5° and 43.5° can be clearly observed, which correspond to an amorphous carbon framework.[6] For the Mo₂C/OMC sample, intense diffraction peaks at 34.5°, 37.9°, 39.5°, 52.2°, 61.7°, 69.6°, 74.8°, and 75.7° are attributed to the structure of Mo₂C (JCPDS 00-011-0680), indicating the formation of well-crystallized Mo₂C. Different from the Mo₂C/OMC, the MoC–OMC only yielded poorly resolved diffraction peaks centered at around 34.9°, 36.6°, 39.2°, and 61.6°, which can be approximately ascribed to a MoC (JCPDS 01-089-4305) crystalline phase. The very broad and poorly resolved diffraction peaks suggest that the MoC was poorly crystallized or its crystal size was very small. To verify the formation of the MoC phase by this one-pot method, we increased further the Mo content and observed very sharp MoC diffraction peaks (see Fig. S1†), confirming that the broad and poorly resolved XRD peaks in Fig. 1b were due to very small MoC particle sizes. It is known that MoC is less stable compared with Mo₂C, therefore, only Mo₂C is formed by the conventional temperature-programmed CH₄/H₂ reaction on oxide supports[1b,9] or by carbothermal reduction on carbon supports.[2] Clearly, our present one-pot co-operative self-assembly synthesis method, when combined with the carbothermal reduction procedure, could result uniquely in the formation of the MoC–OMC composite.
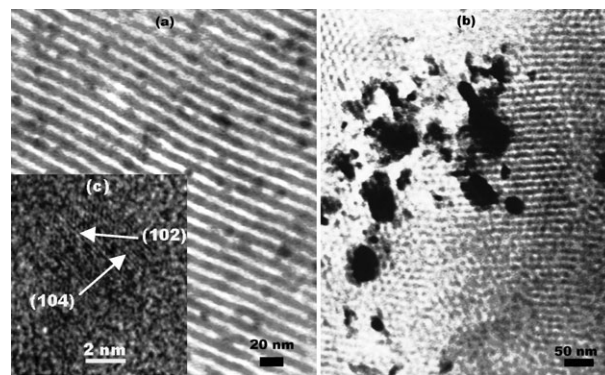


**Fig. 2** TEM images of (a) MoC–OMC, (b) Mo₂C/OMC and (c) HRTEM images of MoC–OMC.

The TEM images in Fig. 2a clearly show the presence of ordered mesoporous structure with pore sizes of ∼6 nm and pore wall thickness of ∼7 nm. Furthermore, it can be seen that the MoC particles having uniform sizes of 3–5 nm are highly dispersed and imbedded in the pore walls of the carbon structure. The TEM image of the MoC–OMC viewed along the [001] direction confirms that the MoC nanoparticles were not included in the pores with hexagonal arrangement, but imbedded in the walls (see Fig. S2†). Moreover, from the HRTEM image, one can clearly see the lattice fringes with d spacing of 2.13 and 2.39 Å, which correspond, respectively, to the [104] and [102] planes of the MoC nanocrystals. These results are in good agreement with the XRD determinations. On the contrary, the TEM image of the Mo₂C/OMC shows that very large Mo₂C particles were formed on the surface of the OMC, while the ordered mesostructures of carbon was partially destroyed. This demonstrates that post-impregnation followed by carbothermal reduction will cause severe aggregation/agglomeration of the Mo₂C nanoparticles, while our present one-pot co-operative organic–organic self-assembly method can result in the imbedding of small nanoparticles into the carbon walls, thus limiting greatly the growth of the nanoparticles under severe pyrolyzing conditions. For the synthesis of ordered mesoporous carbons, the formation of hydrogen bonding between the phenolic resin and the surfactant has been well understood,[8f] which is the key factor for the self-assembly and formation of ordered mesoporous structures. With the introduction of the Mo₇O₂₄⁶⁻ to the reaction mixture, the Mo₇O₂₄⁶⁻ will probably form complexes with the phenolic resin *via* oxygen bridges to form Mo-containing polymers, as indicated by the green color of the polymer (see Fig. S3†). After pyrolysis, the resin polymer was converted into the carbon framework and the Mo ions were reduced by the carbon framework and/or the emitted reducing gas (*e.g.*, CO) to form MoC nanoparticles, which were imbedded in the carbon walls. On the other hand, the micells of the surfactant F127 were decomposed to form the pores of the mesoporous structure.

Nitrogen adsorption–desorption isotherms are very similar for the three samples (Fig. 3), showing representative type IV isotherms with H₂ hysteresis loops, which are typical of mesoporous structure. In addition, the three materials also contained micropores. Micropore volume calculated from the *t*-plot was 0.15 cm³ g⁻¹ for all the three samples (Table S1†). The pore size distributions are narrow, centered at 5.4, 5.5 and 4.6 nm for OMC,
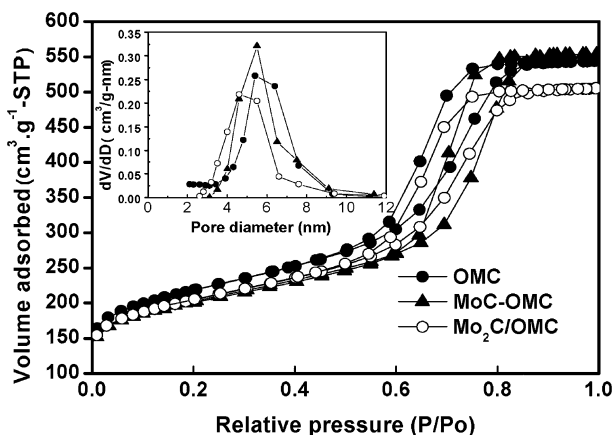
**Fig. 3** Nitrogen adsorption–desorption isotherms for OMC, MoC–OMC and Mo$_2$C/OMC. Inset is the pore size distributions of the three samples.



**Fig. 4** N$_2$H$_4$ conversions *versus* reaction temperature over MoC–OMC, Mo$_2$C/AC and Mo$_2$C/OMC.

MoC–OMC and Mo$_2$C/OMC, respectively. It should be noted that after the incorporation of the MoC or the supporting of the Mo$_2$C, the BET surface area was only slightly decreased, from 758 m$^2$ g$^{-1}$ to 700 m$^2$ g$^{-1}$ (Table S1†). This result is also consistent with the fact that MoC was imbedded into the carbon walls, while Mo$_2$C was merely supported on the outer surface of the carbon, so that the mesopores and micropores were not blocked by the molybdenum carbide particles in either case. This will facilitate mass transfer during the reaction on the one hand, and ensure accessibility of the reactant molecules on the other hand.

Subsequently, catalytic performance of the MoC–OMC composite was evaluated for the hydrazine decomposition, which is an important reaction for attitude control of spacecrafts.[10] The reaction was carried out in a fixed-bed microreactor under atmospheric pressure. 50 mg of a catalyst sample was diluted with 200 mg of inert quartz sand, and placed in a U-shaped quartz reactor. Prior to the reaction, the catalyst was pre-reduced with pure H$_2$ at 773 K for 1 h. N$_2$H$_4$ (3 v/v%) in Ar was allowed to pass through the catalyst bed at a flow rate of 85 ml min$^{-1}$ (GHSV = 51 000 per h). The Mo loading of the investigated samples were basically the same (4 wt%). As shown in Fig. 4, N$_2$H$_4$ conversion over the MoC–OMC attained 100%, even at 30 °C. In contrast, it was only 25% at 30 °C and it reached 100% at 70 °C over the Mo$_2$C/OMC. For comparison, amorphous carbon (Norit, S$_{BET}$ = 1200 m$^2$ g$^{-1}$) was also used as the support of Mo$_2$C, and the resultant Mo$_2$C/AC catalyst also showed a low activity. Evidently, our one-pot prepared MoC–OMC catalyst exhibited the best catalytic performance among the three samples, and it was even more active than our previously reported Mo$_2$C/Al$_2$O$_3$.[10b] We further compared the MoC–OMC with pure Mo$_2$C, and calculated their reaction rates at 30 °C. It was found that the reaction rate over the MoC–OMC was 162 moles N$_2$H$_4$ converted per mole Mo per hour, which is approximately 6 times larger than that on the pure Mo$_2$C. Two features are supposed to be responsible for the enhanced activity of the MoC–OMC: the highly dispersed MoC nanoparticles and the formation of the MoC phase, both of which were a result from the one-pot co-operative organic–organic self-assembly method.

In summary, we have developed a one-pot method for fabricating MoC–OMC nanocomposite, in which very small MoC nanoparticles are highly disperse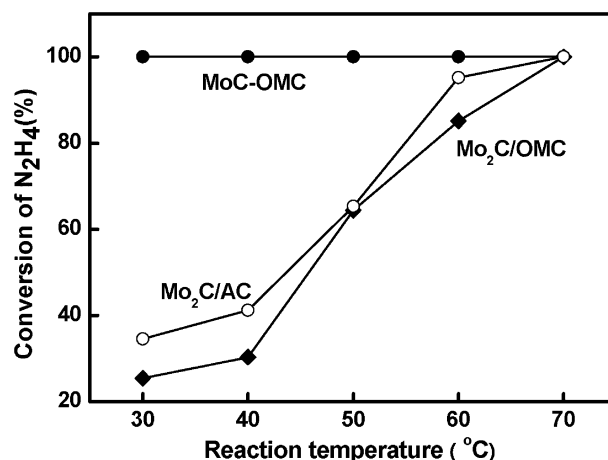d and imbedded in the carbon walls of ordered mesoporous carbons. Preliminary tests have shown that the MoC–OMC composite exhibited excellent performance for N$_2$H$_4$ decomposition. This one-pot method can be extended to other carbide–OMC composites, and the unique features and advantages of the resultant composites are worth further exploring.

## Notes and references

1 (a) S. T. Oyama, *Catal. Today*, 1992, **15**, 179; (b) X. W. Chen, T. Zhang, P. L. Ying, M. Y. Zheng, W. C. Wu, L. G. Xia, T. L i, X. D. Wang and C. Li, *Chem. Commun.*, 2002, 288; (c) R. Barthos, A. Széchenyi, Á. Koós and F. Solymosi, *Appl. Catal., A*, 2007, **327**, 95.
2 (a) C. H. Liang, W. P. Ma, Z. C. Feng and C. Li, *Carbon*, 2003, **41**, 1833; (b) X. Y. Li, D. Ma, L. M. Chen and X. H. Bao, *Catal. Lett.*, 2007, **116**, 63.
3 C. H. Liang, P. L. Ying and C. Li, *Chem. Mater.*, 2002, **14**, 3148.
4 (a) S. M. Holmes, P. Foran, E. P. L. Roberts and J. M. Newton, *Chem. Commun.*, 2005, 1912; (b) W. C. Choi, S. I. Woo, M. K. Jeon, J. M. Sohn, M. R. Kim and H. J. Jeon, *Adv. Mater.*, 2005, **17**, 446; (c) P. Krawiec, E. Kockrick, P. Simon, G. Auffermann and S. Kaskel, *Chem. Mater.*, 2006, **18**, 2663.
5 A. H. Lu, W. C. Li, Z. S. Hou and F. Schüth, *Chem. Commun.*, 2007, 1038.
6 F. B. Su, F. Y. Lee, L. Lv, J. J. Liu, X. N. Tian and X. S. Zhao, *Adv. Mater.*, 2007, **17**, 1926.
7 (a) R. Ryoo, S. H. Joo and S. Jun, *J. Phys. Chem. B*, 1999, **103**, 7743; (b) S. Jun, S. H. Joo, R. Ryoo, M. Kruk, M. Jaroniec, Z. Liu, T. Ohsuma and O. Terasaki, *J. Am. Chem. Soc.*, 2000, **122**, 10712; (c) J. S. Lee, S. H. Joo and R. Ryoo, *J. Am. Chem. Soc.*, 2002, **124**, 1156.
8 (a) C. D. Liang, K. L. Hong, G. A. Guiochon, J. W. Mays and S. Dai, *Angew. Chem., Int. Ed.*, 2004, **43**, 5785; (b) S. Tanaka, N. Nishiyama, Y. Egashira and K. Ueyama, *Chem. Commun.*, 2005, 2125; (c) Y. Meng, D. Gu, F. Q. Zhang, Y. F. Shi, H. F. Yang, Z. Li, C. Z. Yu, B. Tu and D. Y. Zhao, *Angew. Chem., Int. Ed.*, 2005, **44**, 7053; (d) F. Q. Zhang, Y. Meng, D. Gu, Y. Yan, C. Z. Yu, B. Tu and D. Y. Zhao, *J. Am. Chem. Soc.*, 2005, **127**, 13508; (e) F. Q. Zhang, Y. Meng, D. Gu, Y. Yan, Z. X. Chen, B. Tu and D. Y. Zhao, *Chem. Mater.*, 2006, **18**, 5279; (f) C. D. Liang and S. Dai, *J. Am. Chem. Soc.*, 2006, **128**, 5316; (g) C. Y. Liu, L. X. Li, H. H. Song and X. H. Chen, *Chem. Commun.*, 2007, 757.
9 (a) M. Nagai, K. Oshikawa, T. Kurakami, T. Miyao and S. Omi, *J. Catal.*, 1998, **180**, 14; (b) A. D. Consuegra, P. M. Patterson and M. A. Keane, *Appl. Catal., B*, 2006, **65**, 227.
10 (a) R. H. Cheng, Y. Y. Shu, M. Y. Zheng, L. Li, J. S, X. D. Wang and T. Zhang, *J. Catal.*, 2007, **249**, 397; (b) X. W. Chen, T. Zhang, M. Y. Zheng, L. G. Xia, T. Li, W. C. Wu, X. D. Wang and C. Li, *Ind. Eng. Chem. Res.*, 2004, **43**, 6040; (c) X. W. Chen, T. Zhang, M. Y. Zheng, Z. L. Wu, W. C. Wu and C. Li, *J. Catal.*, 2004, **224**, 473.